Int J Clin Exp Med 2017;10(1):385-393
www.ijcem.com /ISSN:1940-5901/IJCEM0039179

Original Article

Mismatch in size of occluding devices for atrial septal defect (ASD) impairs endothelialization of the occluder surface in a canine ASD model

Ge-Sheng Cheng[1], Yu-Shun Zhang[1], Ting-Ting Zhang[1], Chen Wan[2], Xu-Mei He[1], Ya-Juan Du[1]

[1]Department of Cardiology, Xi'an Jiaotong University First Affiliated Hospital, Xi'an, Shaanxi, China; [2]Department of Cardiology, Third Military Medical University Xi Nan Hospital, Chongqing, China

Received August 31, 2016; Accepted October 9, 2016; Epub January 15, 2017; Published January 30, 2017

Abstract: Endothelialization of the atrial septal defect (ASD) occluding device is of major clinical relevance. We aim to identify the effect of occluding devices of different sizes on endothelialization of the occluder surface in a canine ASD model. A 6 mm-diameter circular defect was generated in the center of the oval fossa of 12 dogs. The animals were then randomly assigned to receive an 8 mm-diameter occluder (group A), a 12 mm-diameter occluder (group B) or a 16 mm-diameter occluder (group C). The shape of the occluders and endothelialization of the occluder surface was assessed by different methods. Transthoracic echocardiography (TTE) showed that no occluder dropped off or changed position. Fourteen months after implantation, the occluder surface was completely covered with endothelial tissues in group A, while in group C the occluder surface was covered with islands of endothelial tissues. Immunoblotting assays showed the highest endothelial expression of eNOS in group A (1.21±0.25) followed by group B (0.73±0.18). The nuclei were clearly seen and evenly distributed and tight junctions were observed between endothelial cells in group A on transmission electron microscopy. The occluder surface in group C showed only partial coverage by endothelial tissues and the center of the occluder only showed skeleton of collagen fibers. Transmission electron microscopy showed lack of tight junction between endothelial cells and gaps were present. Oversized occluders show impaired endothelialization of the occluder surface.

Keywords: Atrial septal defect, occluder, endothelialization

Introduction

The use of closure devices for atrial septal defect (ASD) is growing; however, our knowledge concerning the long-term safety and efficacy of these devices still remains rather limited. Rapid endothelialization of ASD occlusion devices after implantation is clinically relevant because it prevents thrombosis by avoiding direct contact between blood and the metal device. Quick and complete endothelialization of a closure device also prevents corrosion of nickel and avoids the position changes of the occluder [1]. It has been known that most ASD repair devices are fully endothelialized within 3-6 months of implantation in animals and endothelial cells are observed as early as 30 days after implantation [2, 3].

However, in our clinical practice, anecdotal cases of incomplete endothelialization were reported [4, 5]. We speculate that incomplete endothelialization may be associated with inappropriate choice of occluder size. In the present study, we established an ASD model in dogs and investigated the endothelialization of ASD occluding devices of different sizes after 14 months of implantation.

Material and methods

Animals and occluders

12 mongrel adult canines, weighing 18-22 kg each, were obtained from the Experimental Animal Center of Xi'an Jiaotong University, Xi'an, China. The study protocol was approved by the Animal Ethics Committee of Xi'an Jiaotong University and the animal study was performed in strict accordance with the institutional and state guidelines on the experimental use of

animals. The occluders were Cardi-O-Fix ASD occluders, which were made of Nickel-titanium wire, imitate structure of Amplatzer occluders and were approved by the State Food and Drug Administration (SFDA) and CE.

Surgical creation of ASD

The dogs were pre-anesthetized with sodium pentobarbital (3 mg, IM) and anesthesia was induced with thiopental (8-12 mg/kg, IV) following IV catheter placement. The dogs were intubated and placed on a surgical table and were maintained on isoflurane (1-3%) inhalation anesthesia for the duration of the procedure. Each animal was monitored by a pulse-oximeter.

A right thoracotomy was performed via a 5 cm incision between the right edge of the sternum and the fourth intercostal space and the heart was exposed. A vertical incision was made in the pericardium, 2 cm anterior and parallel to the right phrenic nerve to allow the right atrium and inferior vena cava to be fully exposed. The right atrial appendage was pressed against the atrial septum and the left index finger was passed through the right atrial appendage to palpate the fossa ovalis, the coronary sinus and the opening of the inferior vena cava for determination of the projection position of these structures onto the surface of the heart. A 4-0 Prolene purse-string suture was placed in the upper edge of the oval fossa. A small hole was created by a sharp knife in the center of the purse-string structure and then a puncher was pushed into the right atrium with the long axis of the puncher perpendicular to the atrial septum. Then, the purse-string was tightened, the sleeve was fixed, and the inner core was pushed. When the puncher reached the atrial septum, it was forcibly twisted and punctured into the left atrium. The push of the inner core was stopped upon loss of resistance when the front of the puncher reached inside the left atrium and the sleeve was pushed along the long axis of the puncher. The atrial septal tissue around the puncture site was fixed between the inner core and the sleeve. The inner core was rapidly retracted into the sleeve, the puncher was removed, and the purse-string was tightened to prevent bleeding. The pericardial incision was repaired, and the chest was closed in layers. A 6 mm-diameter circular defect was generated in this manner in the center of the oval fossa.

ASD closure with occluders

The dogs (n=4 per group) were randomly assigned to receive an 8 mm-diameter occluder (group A), a 12 mm-diameter occluder (group B) or a 16 mm-diameter occluder (group C). After soaking in heparin saline, the occluder was screwed onto the transmission rod, and then loaded into an 8 F long guiding sheath. The sheath was advanced into the right atrium through the hole on the purse-string and pushed into the left atrium through the ASD under transthoracic echocardiography (TTE) guidance. The left disc was deployed first and adjusted to be parallel to the atrial septum, and the sheath was then withdrawn. The waist was released and the right disc was deployed on the other side to occlude the ASD. A to-and-fro motion of the sheath was performed to ensure a secure position across the defect, which was further confirmed by TTE. The transmission rod was turned counterclockwise until the shunt between the left and right atrium disappeared. TTE showed no significant residual shunt, no atrioventricular valve distortion and no obstruction of the coronary sinus. Then, the occluder was released, the sheath was withdrawn and the purse-string structure was tightened. Gentamycin (80000 U) was injected intrathoracically and the chest was closed routinely with placement of a drainage tube.

The vital signs were closely monitored after the operation. Penicillin (3200000 U) was given twice per day for three days and aspirin (5 mg/kg) was given with food daily for 14 months.

Evaluation of the implanted occluders

TTE was performed to evaluate the position and morphology of the occluders and the presence of residual shunt and valvular regurgitation immediately post occluder implantation. Furthermore, 14 months post occluder implantation, the dogs were sacrificed by bloodletting under anesthesia. The heart was removed and the shape of the occluder grossly observed and the thickness of the occluder measured with a vernier caliper. The presence of thrombus or vegetation was observed.

Immunohistochemistry

An S-P Kit (GeneTech, Shanghai) was used for immunohistochemical analysis. Briefly, paraffin sections (4 μm thick) were deparaffinized in xylene and rehydrated in gradient alcohol.

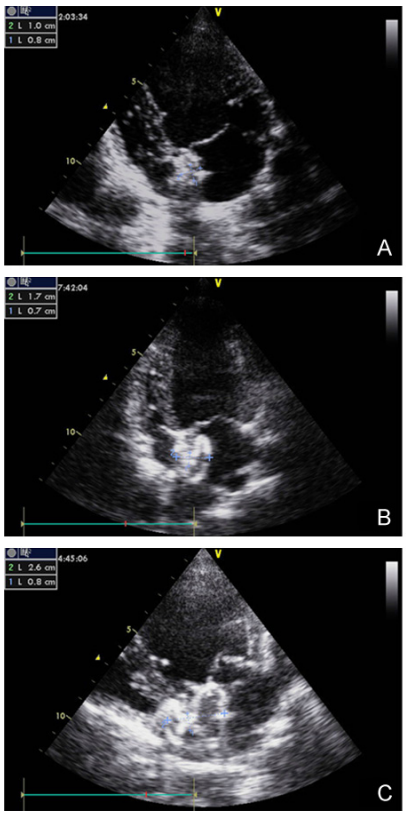

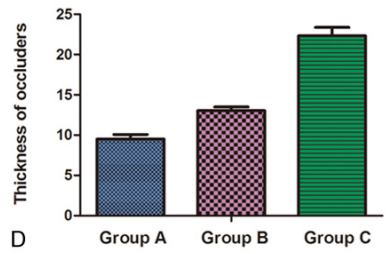

Figure 1. TTE examination showed that six months after surgery, occluders in group A are flat and thin (A), occluders in gourp B are "seashell-shaped" and thicker (B), occluders in group C are "dumbbell-shaped" and thickest (C). Thickness of occluders at six months after surgery are 9.50±0.58 mm in group A, 13.03±0.45 mm in group B and 22.33±1.04 mm in group C (D).

Table 1. Thickness of occluder in each group at different time points (mm)

	Group A	Group B	Group C
Immediately after surgery	10.00±0.32	15.37±1.73	24.33±2.52
Three month after surgery	9.63±0.48	13.37±0.57	22.48±1.06
Six months after surgery	9.50±0.58	13.03±0.45	22.33±1.04
Fourteen months after surgery	10.00±0.40	13.50±0.50	24.00±2.00

Immediately after surgery, Group B compared with Group A, F=29.23, p=0.0009; Group C compared with Group B, F=2.12, p=0.0011. Three months after surgery, Group B compared with Group A, F=1.41, p=0.0001; Group C compared with Group B, F=3.46, p<0.0001. Six months after surgery, Group B compared with Group A, F=1.66, p=0.0001; Group C compared with Group B, F=5.34, p<0.0001. Fourteen months after surgery, Group B compared with Group A, F=1.56, p<0.0001; Group C compared with Group B, F=16.00, p=0.0001.

Antigen retrieval was performed by microwave treatment in 0.01 mol/L sodium citrate buffer (pH=6.0) for 15 min and endogenous peroxidase activity was inactivated with 0.3% hydrogen peroxide for 30 min. Non-specific binding was blocked with avidin/biotin blocking solutions and 10% normal goat serum. The sections were then incubated overnight with primary antibody against eNOS (Santa Cruz Biotechnology, Santa Cruz, CA). Biotinylated goat anti-rabbit IgG was used as secondary antibody. The immunoreactions were detected by staining with 3,3'-diaminobenzidine. Negative controls were performed by omitting the primary antibody. Brown staining by anti-eNOS antibody was considered positive. The number of endothelial cells in 5 randomly selected high-powered (×100) fields per slide was calculated.

Immunoblotting assays

Cellular lysates were prepared in lysis buffer (1% SDS, 50 mM Tris, pH 7.4, 0.15 M NaCl, 1 mM NaF, 10 mM phenylmethylsulfonyl fluoride, 1 mM sodium orthovanadate, and 1 mM EDTA). Proteins were quantified using Bio-Rad DC protein assay (Biorad) and samples were resolved on 4% to 20% SDS denatured polyacrylamide gel. Immunoblotting assays were performed as previously described [4] and anti-eNOS and β-actin antibodies (all from Santa Cruz Biotechnology) were used. Protein bands were visualized using the electrochemiluminescence method and densitometric analysis was carried out using the MCID imaging software (Imaging Research Int., St. Catharines, ON, Canada). Protein expression was normalized against β-actin.

Scanning and transmission electron microscopy

For scanning electron microscopy, the neoendothelium was harvested and fixed with 2% electron microscopy-grade glutaraldehyde for 2 h, post-fixed in 1% osmium tetroxide with 0.1% potassium ferricyanide, dehydrated in gradient ethanol (30-90%), and embedded in Epon. Ultrathin sections (65 nm) were cut, stained with 2% uranyl acetate and examined under a scanning electron microscope (S-3400N,

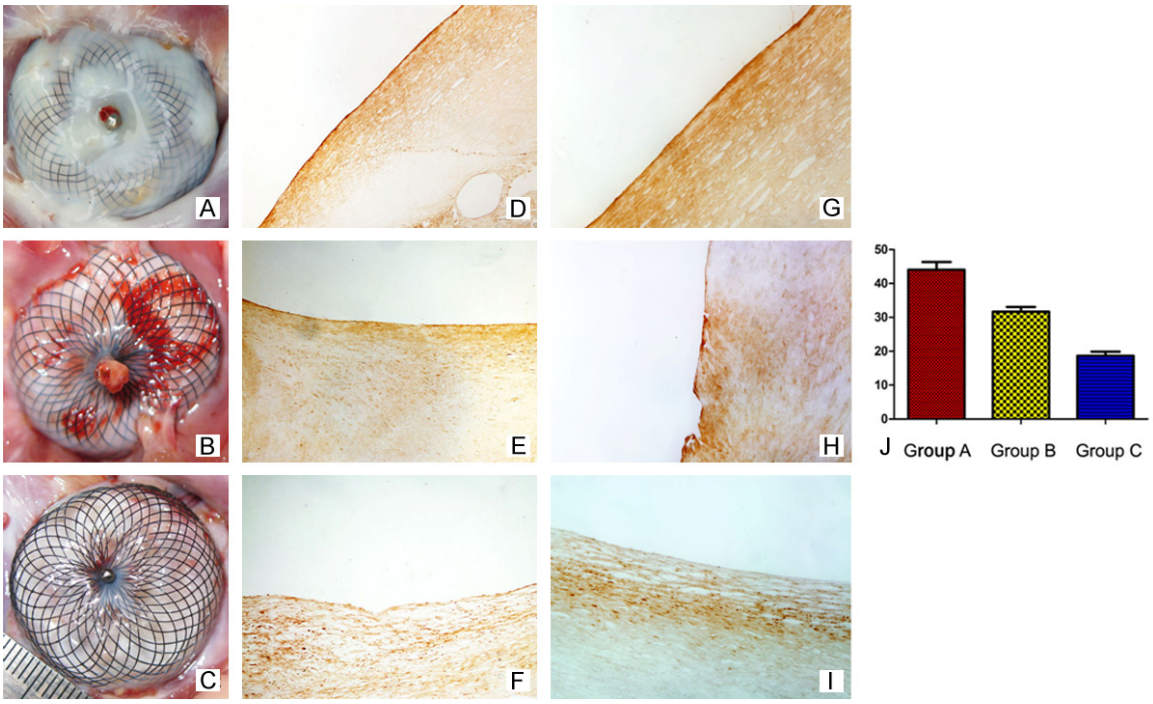

Figure 2. The occluder surface was completely covered with newborn tissues in group A (A) while more than half in group B (B) and with most of bare in group C (C). The cells on the surface of the newborn tissues are positive when they were stained by eNOS antibody, which can be confirmed as neoendothelium (D to I). (D) Neoendothelium in group A, 200X magnification. (E) Neoendothelium in group B, 200X magnification. (F) Neoendothelium in group C, 200X magnification. (G) Neoendothelium in group A, 400X magnification. (H) Neoendothelium in group B, 400X magnification. (I) Neoendothelium in group C, 400X magnification. (J) The mean number of endothelial cells from five randomly chosen fields was the highest in group A (44.00±5.76) and the lowest in group C (18.07±2.94) while the mean number of endothelial cells in group B (31.67±3.39) fell between that of group A and group C (P=0.0102 between group A and group B, P=0.0009 between group B and group C, P=0.0002 between group A and group C).

Hitachi, Tokyo, Japan) with the surface coated with a gold layer transmission electron microscopy (JEM-2100F, Hitachi).

Statistical analysis

Data were expressed as $\bar{x} \pm s$ and analyzed using the SPSS statistical software version 13.0 (SPSS Inc., Chicago, IL). ANOVA analysis was used to compare data between groups. $P<0.05$ was considered statistically significant.

Results

Survival rate

One dog in group C dead about one month after operation, numerous inflammatory cells were observed on the oversized occluder's surface under the microscope, combine with its cough and high temperature before death, we thought the cause of death may be infection. Erosion or malposition did not happen in all occluders.

Morphological characteristics of the implanted occluders

TTE revealed no presence of thrombosis and the distance was more than 5 mm between the edge of the defect and the mitral valve, tricuspid valve, superior vena cava, inferior vena cava, and coronary sinus, meeting the indications for transcatheter closure of ASD. Furthermore, TTE showed that no occluder dropped off or changed position during the study period. Occluders in group A appeared flat and thin, those in group B were seashell-shaped and thicker, and those in group C were dumbbell-shaped and the thickest (**Figure 1** and **Table 1**). No residual shunt was observed in group A and B on color Doppler flow imaging while residual shunt was detected in group C. Macroscopically, 14 months post implantation of the occluder, the occluder surface was completely covered with endothelial tissues in group A (**Figure 2A**) while more than half of the

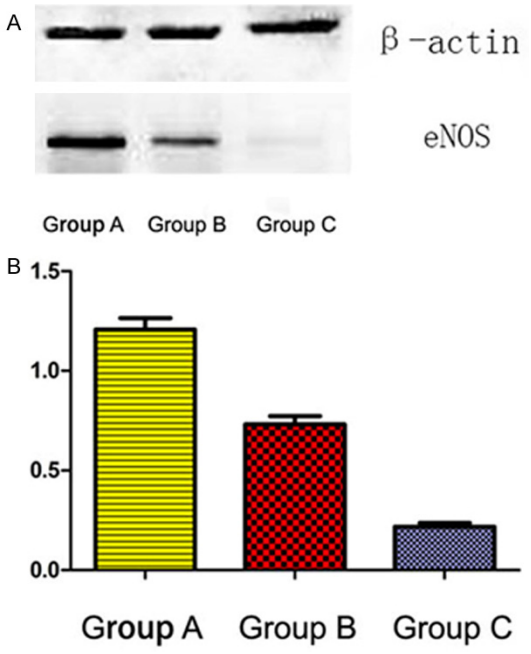

Figure 3. Western blotting assays showed the highest expression of eNOS in the endothelial tissues of the occluder surface in group A (1.21±0.25) followed by group B (0.73±0.18), the lowest eNOS expression was observed in group C (0.22±0.08) (P=0.0207 between group A and group B, P=0.0021 between group B and group C, P=0.0003 between group A and group C).

occluder surface was covered by endothelial tissues in group B (**Figure 2B**). In group C, the occluder surface was covered with islands of endothelial tissues, with most of the occluder surface bare (**Figure 2C**). The identity of the neo-endothelium was confirmed by immunostaining for eNOS (**Figure 2D-I**). Furthermore, the mean number of endothelial cells from five randomly chosen fields was the highest in group A (44.00±5.76) and the lowest in group C (18.07±2.94) while the mean number of endothelial cells in group B (31.67±3.39) fell between that of group A and group C (P<0.05 between groups) (**Figure 2J**). Western blotting assays showed the highest expression of eNOS in the endothelial tissues of the occluder surface in group A (1.21±0.25) followed by group B (0.73±0.18). The lowest eNOS expression was observed in group C (0.22±0.08) (P<0.05 between groups) (**Figure 3**).

Electron microscopic features of the implanted occluders

Endothelial tissues grew differently among groups. The differences among groups, newborn tissues on the center of occluders and at the boundary of occluders can be seen in **Figure 4**.

We further studied the number of newborn endothelial cells and connection between them. The differences among groups can be seen in **Figure 5**.

Then we evaluated the morphology of newborn endothelial cells by transmission electron microscopy. Transmission electron microscopy revealed that most of the newborn tissues were collagen fibers and fibroblasts, and only a layer of endothelial cells was seen on the surface. Endothelial cells grew on the surface and a large nucleus in was present in the center of the cell, and pinocytosis vesicles and tight junctions were observed. We then compared the growth of endothelial cells in the three groups (**Figure 6**).

Discussion

The prevalence of congenital ASD has increased substantially [7]. Transcatheter ASD closure has been largely used today [8, 9], and has gradually replaced surgical repair because it is minimally invasive, has fewer complications and maintains a good quality of life after operation [10, 11]. King and Mills firstly closed ASD by using a transvenous umbrella technique in 1976, who created a precedent for interventional treatment of ASD [12]. Thereafter, different styles of occluders appeared; however, most of them were limited in clinical use because of large delivery sheath, a high incidence of postoperative residual shunt and so on [13]. The advent of Amplatzer occluder in 1997 solved these problems and Amplatzer septal occluder became the most widely used device for percutaneous ASD closure now [14]. Occluders currently used in China are mostly Amplatzer occluders or domestic imitate Amplatzer occluders. Amplatzer occluder provides a higher rate of complete occlusion for small to moderate ASDs [15], and it also can be used for large ASDs [16]. Amplatzer septal occluder is safe and effective in the majority of patients with deficient rims with the exception of inferior-posterior rim deficiency [17]. The imitate Amplatzer occluders we used in our experiment are Cardi-O-Fix ASD occluders from STARWAY MEDICAL TECHNOLOGY. Saritas *et al*. showed that transcatheter ASD occlusion with Cardio-O-Fix septal occluder (CSO) is safe and effec-

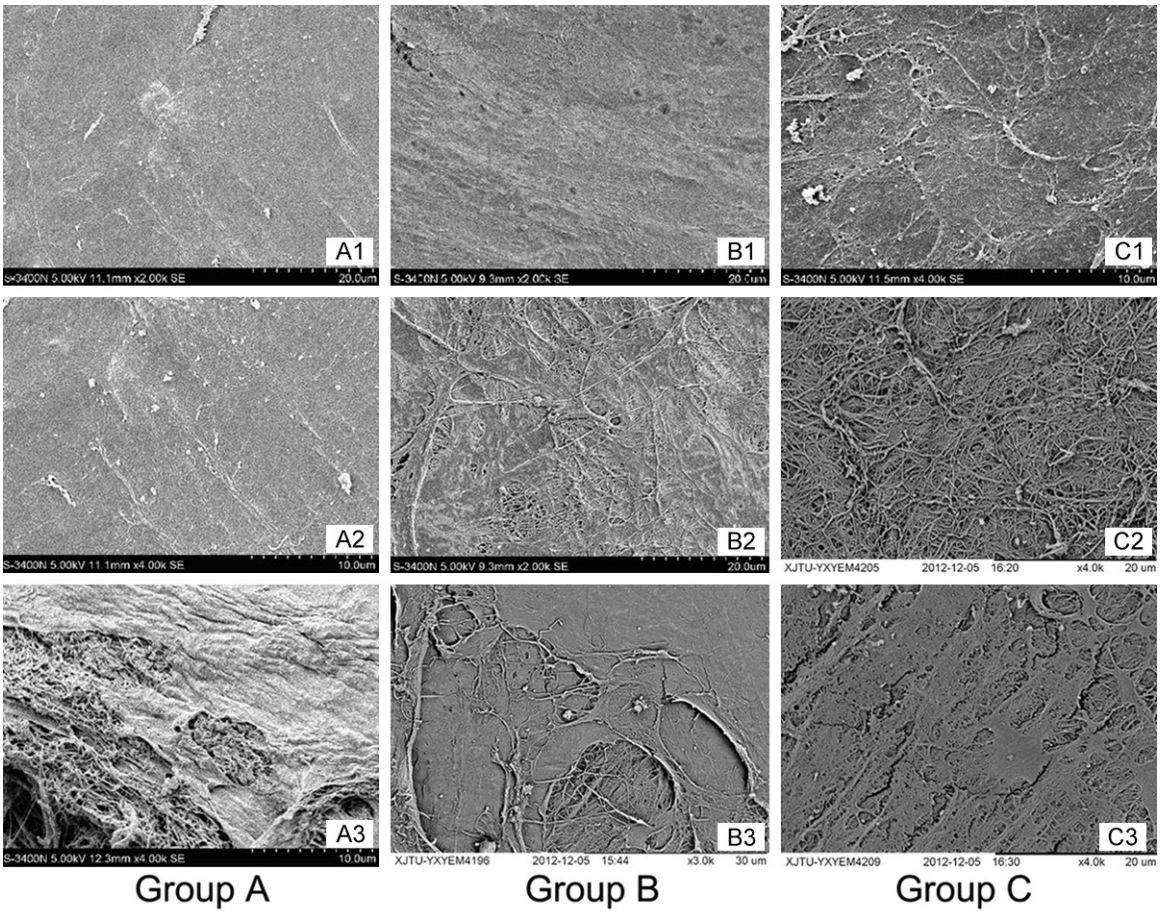

Figure 4. Observing the growth of endothelial cells in three groups by scanning electron microscopy: Endothelial tissues grew thickly and regularly in group A (A1); endothelial tissues grew thinner but also regularly in group B (B1); endothelial tissues grew the thinnest and irregularly in group C (C1). Newborn tissues on the center of occluders: endothelial tissues also grew thickly and regularly in group A (A2), endothelial tissues grew disorderly and incompletely in group B (B2). Furthermore, endothelial tissues were not seen in group C; only collagen fibers were observed (C2). Endothelial tissues at the boundary of complete endothelialization were seen in group A, and only at the edge of the samples collagen fibers were present under the endothelia tissues (A3). Endothelial tissues grew regularly at the boundary in group B (B3) and irregularly at the boundary in group C (C3), and the boundary in group C was closer to the edge of the occluder compared to group B.

tive and it appeared to be an attractive alternative to ASO in closing simple ASD because of its relatively low cost [18].

It has been known that most ASD repair devices are fully endothelialized within 3-6 months of implantation in animals and endothelial cells are observed as early as 30 days after implantation. Howerer, in clinical work these years, Chessa *et al*. reported that an ASD occluder was not fully endothelialized after 18 months of implantation [19]. Sigler *et al*. found that an Amplatzer ASD occluder was covered completely with endothelial tissues one year after implantation, but the endothelial layer was partially very thin [20]. Such pieces of anecdotal evidence suggest that endothelialization of the ASD occluding device is of major clinical relevance. Moreover, with the increasing use of transcatheter therapy of ASD with occluding devices, the structural safety and biocompatibility of occluders has attracted more attention [21, 22].

Newborn tissues gradually grow on the surface of the occluders over time after closure treatment of ASD [23]. Prompt and complete endothelialization of ASD occluding devices is important for a successful outcome of transcatheter therapy of ASD. Delayed or partial endothelialization of ASD occluding devices may be associated with failure of an ASD occluding device or

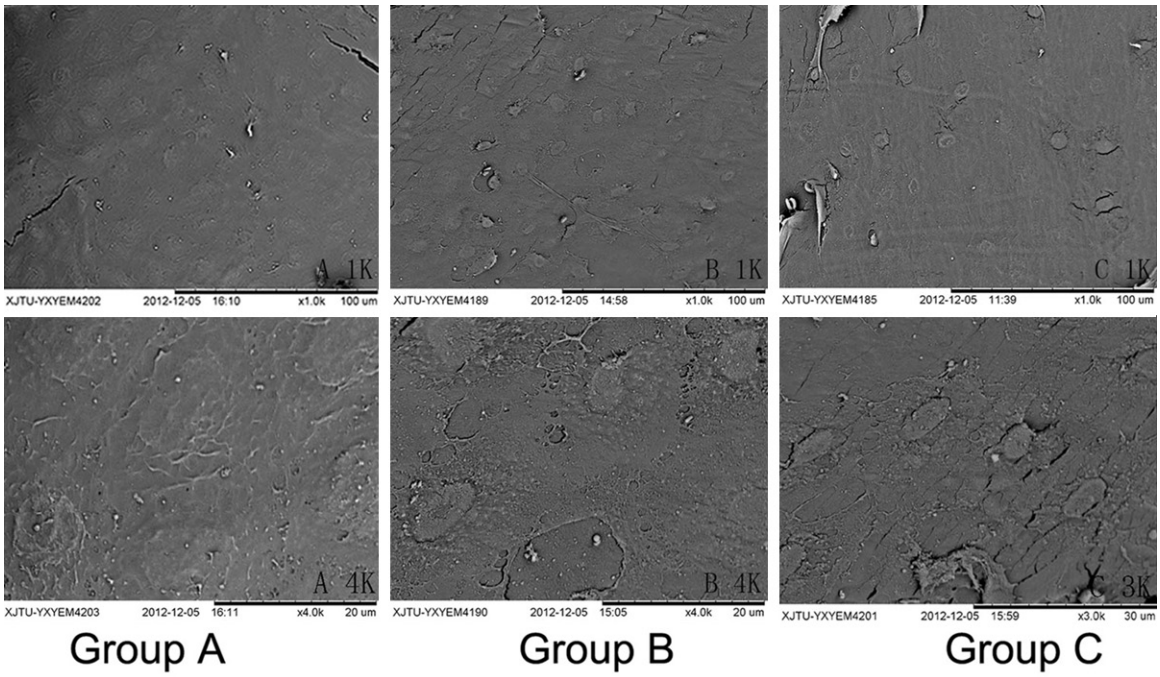

Figure 5. Newborn endothelial cells in three groups seen by scanning electron microscopy: In group A, the number of newborn endothelial cells was the greatest, and the nuclei were evenly distributed and were clearly seen. Tight junctions were observed between endothelial cells. In group B, the number of endothelial cells was between that of group A and group C, and endothelial cells were unevenly distribution. Nuclei were partly seen, and tight junctions were present only among some of the cells. In group C, the number of the endothelial cells was minimum, endothelial cells were unevenly distributed, and only a few nuclei were seen. Gaps were present among most newborn endothelial cells, and tight junctions between cells were hard to spot.

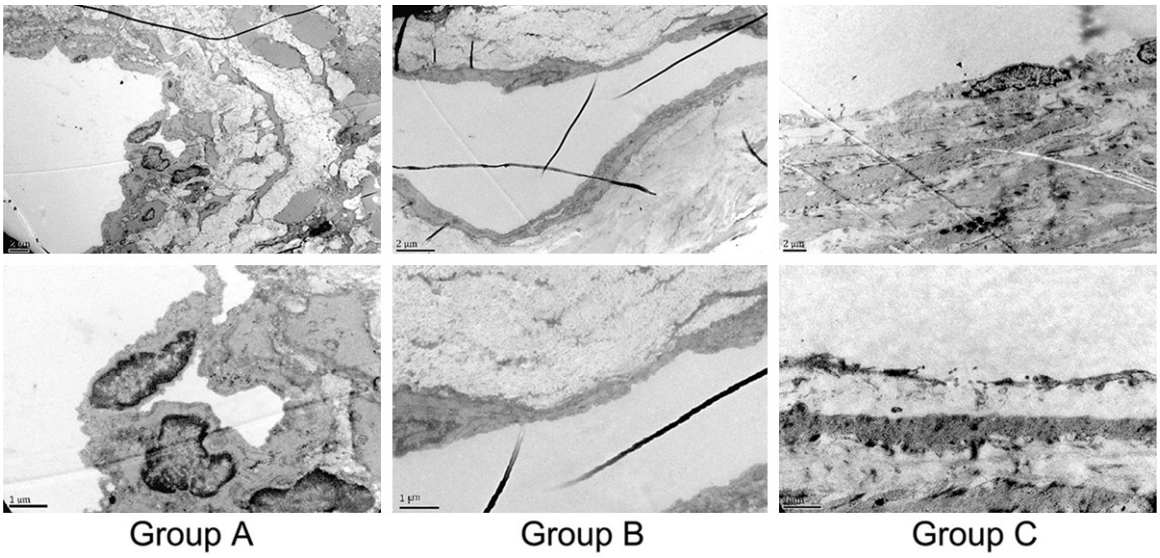

Figure 6. Observing the growth of endothelial cells in three groups by transmission electron microscopy: We could easily find endothelial cells in group A, which grew thick with tight junctions between them. However, it was difficult to find endothelial cells in group B; endothelial cells in group B were thinner than those in group A, but there were many tight junctions between the cells. It was hard to find endothelial cells in group C, and we observed clear gaps between the cells in only 2 samples.

the occurrence of a post implantation complication such as thrombosis, infective endocarditis or malpositioning of the occluding device. Occluders should have stability inside the

human body and allow the growth of endothelial cells.

The degree of endothelialization is not only associated with time, but also may be associated with whether there is a suitable occluder or not [24]. We speculate that the so-called "suitable" means a suitable size, which means incomplete endothelialization may be associated with inappropriate choice of occluder size. In this study we observed the endothelial tissues long-term after closure treatment of ASD, and for the first time confirmed that there existed a relationship between the size of occluder and incomplete endothelialization. We confirmed that we should not choose oversized occluder in order to make sure the successful rate of operations, because when the oversized occluder are implanted, the occluder is pressed by residual atrial septum, what can cause the waist diameter less than its normal size. As a result, the occluder cannot restore its normal shape and will bulge to the heart cavities, and the occluder cannot closely attach to the atrial septum. Endothelial cells consequently cannot grow onto the surface of the occluder. Finally, incomplete endothelialization occurs. This will not only increase the risk of thrombosis, but also increase the possibility of erosion, malposition, infective endocarditis and a variety of other complications. When we choose occluder, we should consider the long-term efficacy for patients, implant an occluder whose diameter is close to the size of the defect, so that the waist of the occluder can easily restore its normal shape, and closely attach to the atrial septum. Finally, endothelial cells can easily grow onto the surface of the occluder. Given increasing worldwide acceptance and utilization of ASD occluding devices, it is important to investigate the long term efficacy and safety of these devices. Our findings demonstrate that choice of an occluding device of appropriate size is critical for endothelialization of the occluder surface in a canine ASD model. This study firstly offers factual basis about how to choose suitable occluder in closure surgery of ASD.

The study has certain limitations. Firstly, the type, size and location of defects are all the same in our experiment, and the surrounding tissue is well developed, and the residual edge is long enough and hard enough, which can provide good support to occluder. This is too idealistic a scenario, while in clinical work, the defects of our patients are varied and at different locations, such as soft edge, lack of edge and porous defects. What's more, our experiment just studied endothelialization on different types of occluders with the same type of defect; however, we did not study the endothelialization on the same type of occluder for defects of different sizes. Furthermore, patients may have an occluder for many years after they have a closure operation, but our dogs just had months, and hemodynamic changes and long-term prognosis still need further elucidation in future experiments.

Disclosure of conflict of interest

None.

Address correspondence to: Dr. Yu-Shun Zhang, Department of Cardiology, Xi'an Jiaotong University First Affiliated Hospital, 76 West Yanta Road, Xi'an 710061, Shaanxi, China. Tel: +86 13991353567; Fax: +86(29) 85324078; E-mail: zys2889@sina.com

References

[1] Hijazi ZM, Hakim F, Al-Fadley F, Abdelhamid J, Cao QL. Transcatheter closure of single muscular ventricular septal defects using the Amplatzer muscular VSD occluder: initial results and technical considerations. Catheter Cardiovasc Interv 2000; 49: 167-172.

[2] Sigler M, Jux C. Biocompatibility of septal defect closure devices. Heart 2007; 93: 444-449.

[3] Sharafuddin MJ, Gu X, Titus JL, Urness M, Cervera-Ceballos JJ, Amplatz K. Transvenous closure of secundum atrial septal defects: preliminary results with a new self-expanding nitinol prosthesis in a swine model. Circulation 1997; 95: 2162-2168.

[4] Zahr F, Katz WE, Toyoda Y, Anderson WD. Late bacterial endocarditis of an amplatzer atrial septal defect occluder device. Am J Cardiol 2010; 105: 279-80.

[5] Chen F, Zhao X, Zheng X, Chen S, Xu R, Qin Y. Incomplete endothelialization and late dislocation after implantation of an Amplatzer septal occluder device. Circulation 2011; 124: e188-9.

[6] Guo J, Chen X, Xi R, Chang Y, Zhang X, Zhang X. AEG-1 expression correlates with CD133 and PPP6c levels in human glioma tissues. J Biomed Res 2014; 28: 388-395.

[7] van der Linde D, Konings EE, Slager MA, Witsenburg M, Helbing WA, Takkenberg JJ, Roos-Hesselink JW. Birth prevalence of congenital heart disease worldwide: a systematic review and meta-analysis. J Am Coll Cardiol 2011; 58: 2241-2247.

[8] Kotowycz MA, Therrien J, Ionescu-Ittu R, Owens CG, Pilote L, Martucci G, Tchervenkov C, Marelli AJ. Long-term outcomes after surgical versus transcatheter closure of atrial septal defects in adults. JACC Cardiovasc Interv 2013; 6: 497-503.

[9] Omeish A, Hijazi ZM. Transcatheter closure of atrial septal defects in children & adults using the Amplatzer septal occluder. J Interv Cardiol 2001; 14: 37-44.

[10] Walters DL, Boga T, Burstow D, Scalia G, Hourigan LA, Aroney CN. Percutaneous ASD closure in a large Australian series: short- and long-term outcomes. Heart Lung Circ 2012; 21: 572-5.

[11] Moake L, Ramaciotti C. Atrial septal defect treatment options. AACN Clin Issues 2005; 16: 252-66.

[12] King TD, Thompson SL, Steiner C, Mills NL. Secundum atrial septal defect. Nonoperative closure during cardiac catheterization. JAMA 1976; 235: 2506-2509.

[13] Zahn EM, Wilson N, Cutright W, Latson LA. Development and testing of the Helex septal occluder, a new expanded polytetrafluoroethylene atrial septal defect occlusion system. Circulation 2001; 104: 711-6.

[14] Bartakian S, El-Said HG, Printz B, Moore JW. Prospective randomized trial of transthoracic echocardiography versus transesophageal echocardiography forassessment and guidance of transcatheter closure of atrial septal defects in children using the Amplatzer septal-occluder. JACC Cardiovasc Interv 2013; 6: 974-980.

[15] Butera G, Carminati M, Chessa M, Delogu A, Drago M, Piazza L, Giamberti A, Frigiola A. CardioSEAL/STARflex versus Amplatzer devices for percutaneous closure of small to moderate (up to 18 mm) atrial septal defects. Am Heart J 2004; 148: 507-510.

[16] Narin N, Baykan A, Argun M, Ozyurt A, Pamukcu O, Bayram A, Uzum K. New modified balloon-assisted technique to provide appropriate deployment in the closure of large secundumatrial septal defect using amplatzer septal occluder in children. J Invasive Cardiol 2014; 26: 597-602.

[17] Fraisse A, Assaidi A, Kammache I, Mancini J, Aldebert P, Luciano D, Ovaert C, Michel N, Habib G. Transcatheter closure of secundum atrial septal defect with deficient rims other than the antero superior using amplatzer devices. JACC 2013; 61: E498.

[18] Saritas T, Kaya MG, Lam YY, Erdem A, Akdeniz C, Demir F, Erol N, Demir H, Celebi A. A comparative study of Cardi-O-Fix septal occluder versus Amplatzer septal occluder in percutaneous closureof secundum atrial septal defects. Catheter Cardiovasc Interv 2013; 82: 116-121.

[19] Chessa M, Butera G, Frigiola A, Carminati M. Endothelialization of ASD devices for transcatheter closure: possibility or reality? Int J Cardiol 2004; 97: 563-564.

[20] Sigler M, Kriebel T, Wilson N. Histological confirmation of complete endothelialisation of a surgically removed Amplatzer ASD occluder. Heart 2006; 92: 1723.

[21] Zhu W, Neubauer H. Secondary residual shunt after atrial septal defect closure with an amplatzer occluder: surgical removal and evaluation of device biocompatibility after 7 years. Pediatr Cardiol 2010; 31: 1107-1110.

[22] Bauriedel G, Skowasch D, Peuster M. Pathology of explanted ASD occluder. Eur Heart J 2007; 28: 684.

[23] Lazarev SM, Agarkova E, Rybakova MG, Antonov NN. The dynamics of morphological alterations in the interatrial septum of the heart in at the occlusion defect of the septum made with the appliance Amplatzer septal occluder. Vestn Khir Im II Grek 2004; 163: 31-34.

[24] Zhang T, Zhang Y, Wan C, Cheng G, Wang J, He X, et al. The effect of oversized occluder on endothelialization after percutaneous closure of experimental atrial septal defect in dogs. Zhonghua Xin Xue Guan Bing Za Zhi 2014; 42: 557-60.